Mem. S.A.It. Vol. 88, 557

Memorie della

Magnetic fields from filaments to cores

P. M. Koch[1], Y.-W. Tang[1], N.L. Chapman[2], A. Duarte-Cabral[3], P.T.P. Ho[1,4], G. Novak[2], N. Peretto[3], Y.-N. Su[1], S. Takakuwa[5,1], and H.-W. Yen[6]

[1] Academia Sinica Institute of Astronomy and Astrophysics (ASIAA), Taipei, Taiwan
e-mail: pmkoch@asiaa.sinica.edu.tw

[2] Center for Interdisciplinary Exploration and Research in Astrophysics (CIERA) and Department of Physics & Astronomy, Northwestern University, USA

[3] School of Physics & Astronomy, Cardiff University, Cardiff, UK

[4] East Asian Observatory (EAO), Hilo, Hawaii, USA

[5] Department of Physics and Astronomy, Graduate School of Science and Engineering, Kagoshima University, Kagoshima, Japan

[6] European Southern Observatory (ESO), Garching, Germany

Abstract. How important is the magnetic (B-) field when compared to gravity and turbulence in the star-formation process? Does its importance depend on scale and location? We summarize submm dust polarization observations towards the large filamentary infrared dark cloud G34 and towards a dense core in the high-mass star-forming region W51. We detect B-field orientations that are either perpendicular or parallel to the G34 filament axis. These B-field orientations further correlate with local velocity gradients. Towards three cores in G34 we find a varying importance between B-field, gravity, and turbulence that seems to dictate varying types of fragmentation. At highest resolution towards the gravity-dominated collapsing core W51 e2 we resolve new B-field features, such as converging B-field lines and possibly magnetic channels.

Key words. ISM: individual objects: (G34, W51) – ISM: magnetic field – Polarization

1. Introduction

The exact role of the magnetic (B-) field in the star-formation process is highly debated. Zeeman observations indicate field strengths that can be comparable to or even dominate over gravity, turbulence or centrifugal force. Simulations predict an evolving role of the B-field with time.

Where and when exactly does the B-field play which role? We summarize B-field observations that cover (1) filamentary scales (several pc) in the infrared dark cloud G34.43+00.24 (hereafter G34) where we trace the large-scale field morphology with a resolution $\theta \sim 10''$ ($\sim$ 0.18pc) and (2) smaller denser cores ($\sim$ 0.05pc) in the high-mass star-forming region W51 where we resolve new B-field structures with $\theta \sim 0\farcs26$ ($\sim$ 5mpc).

We trace the plane-of-sky projected B-field morphology via dust polarization. Dust grains are expected to be aligned with their smaller axes parallel to B-field lines (e.g., Hoang & Lazarian 2016). Emission at (sub-)millimeter wavelengths is, thus, polarized perpendicular to field lines.

2. Results

2.1. Large scales – Filament

The G34 filament extends over about 8pc. Its three most massive cores contain several hundred solar masses each within an area of about 0.5pc. Polarimetric observations with SHARP on the CSO detected the three cores MM1, MM2, and MM3 with a resolution $\theta \sim 10''$ at a wavelength of 350μm. Polarization was clearly detected along and across the filament (Tang et al. 2017). Towards the MM1/MM2 ridge, the B-field is mostly perpendicular to the filament's axis. The B-field appears parallel to the filament around MM3 (Fig. 1). Combining N_2H^+ kinematics (Peretto et al. in preparation) with polarimetric data, we detect a very close alignment between local velocity gradients and local B-field orientations across MM1/MM2. This is suggestive of the B-field guiding the gas flow. A detailed analysis of turbulent-to-mean field, B-field dispersion and B-field strength, turbulent and B-field pressure, virial parameter and mass-to-flux ratio reveals a varying relative importance between B-field (B), gravity (G), and turbulence (Turb) in the three cores. We find G > B > Turb in MM1, B > Turb > G in MM2, and G ~ Turb > B in MM3 (Tang et al. 2017). Interestingly, the three cores display also different fragmentation properties on the next smaller scales (Fig. 1). MM1 shows no fragmentation, consistent with our finding that gravity dominates over both the B-field and turbulence. MM2 displays an aligned fragmentation, likely due to a strong B-field dictating the locations of the fragments. MM3 reveals a clustered fragmentation resulting from a significant level of turbulence. Hence, we propose that the relative importance between B, G, and Turb is responsible for different fragmentation scenarios.

2.2. Small scales – Core

With an improvement in resolution by a factor of about 7 in area over the SMA observations (Tang et al. (2009); $\theta \sim 0''.7$ at 345 GHz), the first ALMA polarization observations towards W51 (Koch et al. (2017); $\theta \sim 0''.26$ at 230 GHz) reveal several new features. ALMA's sensitivity enables a complete polarization coverage, clearly detecting and resolving B-field structures in polarization holes in earlier (less sensitive) SMA data (Fig. 2). The bow-shock shaped B-field structure in the northwestern satellite core suggests that this core is falling towards the central more massive core. Around a southeast-northwest axis starting from the central peak, the field lines appear to symmetrical converge towards a narrow straight line. This striking symmetry (also observed in several regions in W51 e8 and North,

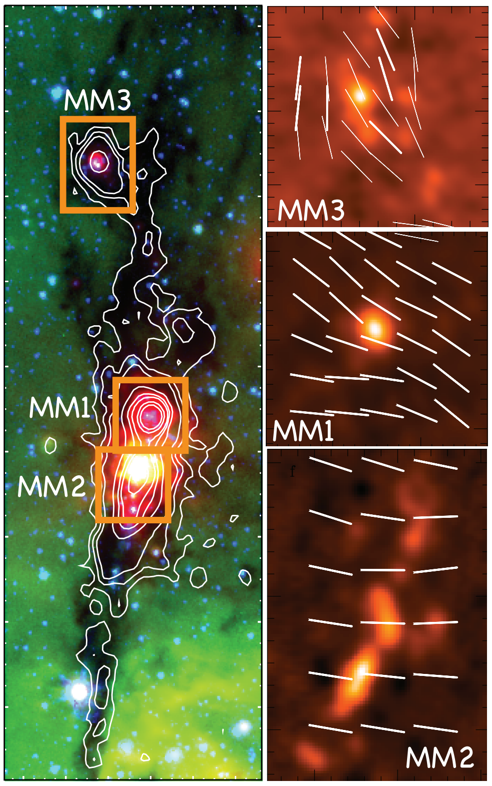

Fig. 1. Left panel: G34 three-color composite map from *Spitzer* (IRSA archive). Contours are 1mm (Rathborne et al. 2006). B-field segments detected with CSO/SHARP at 350μm are shown with white segments in the right panels. Color shows the different fragmentation types, clustered fragmentation in MM3, no fragmentation in MM1, aligned fragmentation in MM2, from higher-resolution observations (Hull et al. 2014; Zhang et al. 2014).

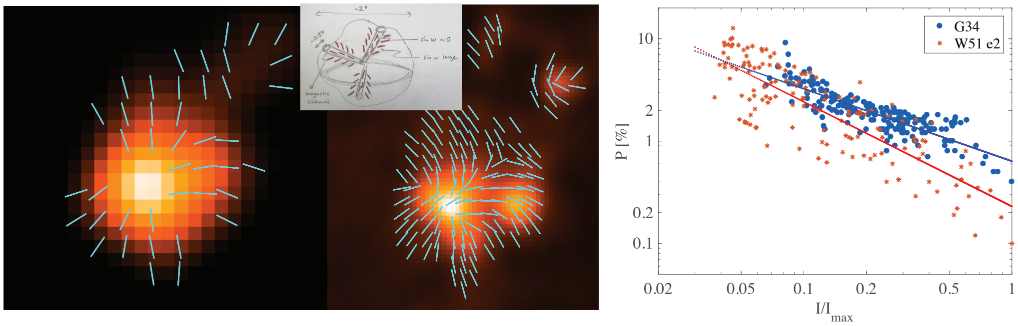

Fig. 2. W51 e2 observed with the SMA (Tang et al. 2009) with a resolution $\theta \sim 0\farcs7$ (left panel) and with ALMA (Koch et al. 2017) with $\theta \sim 0\farcs26$ (middle panel). The color scale is dust continuum. Segments indicate B-field orientations. The ALMA map reveals new sub-structures such as, e.g., the bow-shock shaped B-field morphology in the satellite core in the northwest and the B-field lines symmetrically converging from two sides into a narrow straight line along a southeast-northwest direction starting from the center. The inlet is a cartoon of the envisioned magnetic channels where material can collapse ($\sin\omega \sim 0$) while outside of the channels the B-field provides maximal resistance against gravity ($\sin\omega$ large). Right panel: different slopes, −0.7 for G34 and −1 for W51 e2, for the intensity-vs-polarization percentage correlation.

Koch et al. 2017) has led to the speculation of B-field convergence zones that result in magnetic channelling (Fig. 2). To further quantitatively assess the role of the B-field on small scales in (collapsing) cores we propose a new diagnostic: the $\sin\omega$ measure.

By projecting the direction of the local field tension force onto the direction of gravity, the effectiveness of the B-field to oppose gravity can be assessed. The angle ω between these two directions is measurable from polarization observations. $\sin\omega$ in the range between 0 and 1 measures the fraction of the field tension force that can work against gravity (Koch et al. 2017).

If the two directions are aligned, i.e., $\sin\omega \sim 0$, the B-field cannot slow down gravity. The B-field can maximally oppose gravity when the directions are largely misaligned ($\sin\omega \sim 1$; Fig. 2, inlet). The possible existence of magnetic channels together with the $\sin\omega$ measure has an interesting application. One $0\farcs15$ magnetic channel comprises 0.4% of the entire mass in a $2''$-diameter sphere. A network of 10 channels can then reduce the star-formation rate to 4%, assuming that the mass inside the channels is converted into stars while the material outside is held back by the B-field.

3. Conclusions

Combining polarimetric and kinematics data we quantify B-field, gravity, and turbulence towards three cores in the G34 filament. We conclude that the interplay between these forces varies. Hence, the field can play a role from dominant to negligible. The varying relative importance between these forces seems to be responsible for how fragmentation proceeds. In denser cores in W51 we possibly start to resolve B-field convergence zones that lead to narrow magnetic channels where only a small amount of gas can collapse. Different slopes in the intensity-vs-polarization percentage correlation, −0.7 for G34 and −1 for W51 e2 (Fig. 2, right panel), hint different dust grain properties.

References

Hoang, T. & Lazarian, A. 2016, ApJ, 831, 159H
Hull, C.L.H., et al. 2014, ApJS, 213, 13
Koch, P. M., et al. 2017, ApJ, submitted
Rathborne, J.M., et al. 2006, ApJ, 641, 389
Tang, Y.-W., et al. 2009, ApJ, 700, 251
Tang, Y.-W., et al. 2017, ApJ, submitted
Zhang, Q., et al. 2014, ApJ, 792, 116